Ultraviolet reflectance and electronic states of layered nickel halides studied with synchrotron radiation

I. Pollini
Dipartimento di Fisica, Università degli Studi di Milano and Gruppo Nazionale di Struttura della Materia del Consiglio Nazionale delle Ricerche, I-20133, Milano, Italy
and Laboratoire d'Utilisation du Rayonnement Electromagnétique, Université de Paris—Sud, F-91405 Orsay, France

J. Thomas, G. Jézéquel, and J. C. Lemonnier
Laboratoire de Spectroscopie (Equipe de Recherche No. 748 associée au Centre National de la Recherche Scientifique), Université de Rennes I, F-35010 Rennes, France
and Laboratoire d'Utilisation du Rayonnement Electromagnétique, Université de Paris—Sud, F-91405 Orsay, France

A. Lenselink
Laboratory of Inorganic Chemistry, State University of Groningen, 9747-AG Groningen, The Netherlands
and Laboratoire d'Utilisation du Rayonnement Electromagnétique, Université de Paris—Sud, F-91405 Orsay, France
(Received 20 June 1983)

The real (ϵ_1) and imaginary (ϵ_2) parts of the dielectric function, together with the energy-loss function, $-\mathrm{Im}[1/\hat{\epsilon}(E)]$, of freshly cleaved crystals of $NiCl_2$, $NiBr_2$, and NiI_2 have been obtained in the region 2—31 eV by Kramers-Kronig analysis of near-normal-incidence reflectance spectra. The spectra of NiI_2 have been obtained over the entire region at 300 and 30 K, and those of $NiCl_2$ and $NiBr_2$ have been measured at 30 K only from 2 to 11 eV. The results can be described in terms of charge-transfer transitions, interband transitions, and plasma oscillations. The low-temperature spectra of the materials reveal the presence of exciton structures. Plasma resonance effects have been identified in the high-energy region (15—20 eV). The optical spectra of NiX_2 (X=Cl,Br,I) were analyzed in terms of the known band structures of $NiCl_2$ and $NiBr_2$. Nearly all of the main spectral features beyond the energy gap can be identified in terms of direct interband transitions at the symmetry points Γ, Z, F, and L and along symmetry lines of the Brillouin zone. The energy gap is assigned to $\Gamma_3^- \rightarrow \Gamma_1^+$ transitions in $NiCl_2$ (8.72 eV), $NiBr_2$ (7.90 eV), and NiI_2 (6.26 eV). Finally, the interpretation of the satellite exciton at 5.65 eV in NiI_2 (30 K) and at 6.50 eV in $NiBr_2$ (30 K) is discussed in terms of the triplet exciton state predicted by Onodera and Toyozawa.

I. INTRODUCTION

In the last decade an increasing number of optical measurements have been carried out on transition-metal halides (TMH's) in the vacuum-ultraviolet region (vuv).[1—5] In particular, thin-film transmission measurements on transition-metal chlorides (TMC's) and bromides (TMB's) have included work as far as 40 eV at liquid-nitrogen temperature.[1,2] Fundamental reflectance spectra of single crystals of NiX_2, and of FeX_2 and CoX_2 (X=Cl,Br) (Ref. 4) have recently been taken with the use of synchrotron radiation. These spectra show well-resolved structures which are often sharper than those observed in films at comparable temperatures. This fact indicates that some of the band broadening in films is caused by their structures, which are less ordered than that of bulk crystals. Yet, the observed structures in the reflectance of TMC's and TMB's (Ref. 4) present, in general (but not always), good correspondence with the spectral features found in evaporated films[1,2] in the low-energy ultraviolet region up to 9—10 eV. The electronic transitions in the higher-energy region, however, have neither been extensively studied nor understood. For instance, definite assignments of the peaks around 17 and 23 eV in TMH's,[2] and peaks at 17.8 eV in NiO or 17.5 eV in CoO (Ref. 6), have not been given yet. Concerning iodide compounds, while one finds some detailed experimental information for the absorption-edge structure of binary compounds such as CdI_2,[7,8] HgI_2,[9,10] and PbI_2,[11] optical measurements on transition-metal iodides (TMI's) have been obtained only on crystalline CoI_2 and NiI_2,[12] over a restricted energy range around the lowest-energy edge ($\sim$5 eV), or on evaporated films as far as 6—7 eV, viz., in MnI_2 and FeI_2.[13] Thus further research on these ionic materials is needed, particularly in order to study the structures both below and above the forbidden energy gap, where sharp, intense peaks occur. Furthermore, TMH's are, in general, more ionic than transition-metal oxides and sulfides, and thus phenomena to be interpreted in terms of exciton creation are expected to be more dominant in halides. For these reasons, we have decided to study anew the exciton and interband region in NiI_2, and also extend our previous measurements on $NiCl_2$ and $NiBr_2$ to energies up to 31 eV.

After a brief description of the experimental techniques and sample preparation (Sec. II), we present, in Sec. III,

the reflectance spectra of nickel halides along with the conclusions which follow directly from the experimental results. In particular, values for the imaginary part of the dielectric constant $\epsilon_2(E)$, and the energy-loss function $-\mathrm{Im}[1/\hat{\epsilon}(E)]$, are presented. It is known that the structure of $\epsilon_2(E)$ can be related directly to singularities in the joint density of states for interband transitions,[14] and that the energy-loss function describes the energy loss of fast electrons passing through the material.[15,16]

The marked similarities among the spectra of NiX_2, coupled with the considerable amount of information available on alkali halides,[17–22] make it possible to give quite a reasonable interpretation of the present experimental results. Recent self-consistent band-structure calculations on TMH's (Refs. 23 and 24) and $NiBr_2$,[23] and various soft-x-ray—absorption[25–27] and photoemission[28–30] spectra of TMH's, lend further support to the general picture. Finally, following the known band calculations and basing our analysis on the experimental information, we shall propose, in Sec. IV, a common band structure for NiX_2, which should describe satisfactorily the low-lying electronic transitions in terms of excitons and interband transitions at different points in the Brillouin zone.

II. EXPERIMENTAL TECHNIQUES

Ultraviolet radiation at photon energies between 2 and 31 eV was provided by the 0.54-GeV-electron storage ring of the Laboratoire d'Utilisation du Rayonnement Electromagnétique (Orsay, France). This source is extremely stable in time, since the number of stored electrons decays slowly and steadily over several hours. The radiation was dispersed by means of a Jobin-Yvon holographic grating in an evacuated momochromator (10^{-10} mm Hg) which presents an average resolution of 4–6 Å over the energy range covered. The incident and reflected intensities were measured by means of both EMI-9526 S and Hamamatsu-R268 photomultipliers, provided with a sodium salicylate phosphor. Data were taken at near-normal incidence ($<20°$). Further details on the light source and the experimental apparatus have been given elsewhere.[4]

Single crystals of $NiCl_2$ and $NiBr_2$ have been obtained from the vapor phase by the dynamical-transport method. Direct chlorination and bromination of the nickel powder (Merck, 99.9% pure) at 700 and 600 °C gives gold-yellow ($NiCl_2$) and yellow-brown ($NiBr_2$) crystalline flakes, respectively, which are slightly hygroscopic.[3] Single crystals of NiI_2 have been prepared from the elements using nickel powder (Koch-Light, purity better than 99.99%) and iodine which was sublimed twice (Merck, purity better than 99.5%). The growth of black, shiny crystals of NiI_2 was carried out in two different ways: (i) with a Bridgman method, and (ii) by chemical transport from the elements in a sealed ampoule with a thermal gradient of 650–750 °C.[31] Because all the crystals are hygroscopic, samples were cleaved in a glovebox filled with dry nitrogen and directly attached to the reflectometer. These precautions are necessary in ultraviolet reflectance measurements because the surface condition of the crystal sample is extremely critical, since, in the spectral region of intrinsic absorption, the radiation penetration depth is only a few hundred Å. The use of freshly cleaved surfaces minimizes the probability of obtaining reflectance not intrinsic to the material observed. In this way, measurements on a given sample were reproducible to within 5–10%.

III. EXPERIMENTAL RESULTS AND CONSIDERATIONS

The reflectance spectra of layered nickel halide crystals in the energy region 2–31 eV are shown in Figs. 1–3 together with the spectral dependence of the real and imaginary parts of the dielectric function, $\epsilon_1(E)$ and $\epsilon_2(E)$, and the energy-loss function $-\mathrm{Im}[1/\hat{\epsilon}(E)]$. The gross features of the NiX_2 spectra are very similar below 10–11 eV, where quite a number of strong peaks and features (A–F) are observed (see Fig. 4). Beyond 14–15 eV, however, the spectral profile is very simple; two bands (M and N) are observed in $NiCl_2$: the first one (M) is centered around 18 eV and the second, a very weak one, is centered around 23 eV. Only one band is observed in $NiBr_2$ (M) and NiI_2 (M), around 17 and 14–15 eV, respectively. In the high-energy region, the optical profile shows a smooth decrease which is reminiscent of the behavior of both ionic[20] and partially ionic[19] crystals. In correspondence with this characteristic behavior of the reflectivity, which denotes the region of plasma effects, we can follow the plots of $\epsilon_1(E)$ and $\epsilon_2(E)$ and $-\mathrm{Im}[1/\hat{\epsilon}(E)]$. The latter function exhibits weak structures in the vicinity of the lower-energy peaks and a broader, stronger maximum,

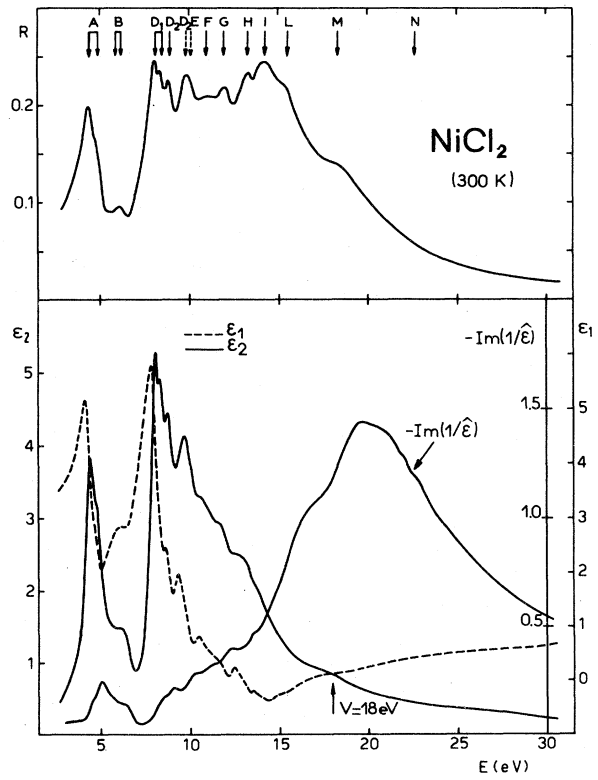

FIG. 1. Spectral dependence of the reflectance R, the real and imaginary parts of the dielectric constant ϵ_1 and ϵ_2, and the energy-loss function $-\mathrm{Im}(1/\hat{\epsilon})$ for $NiCl_2$ at room temperature.

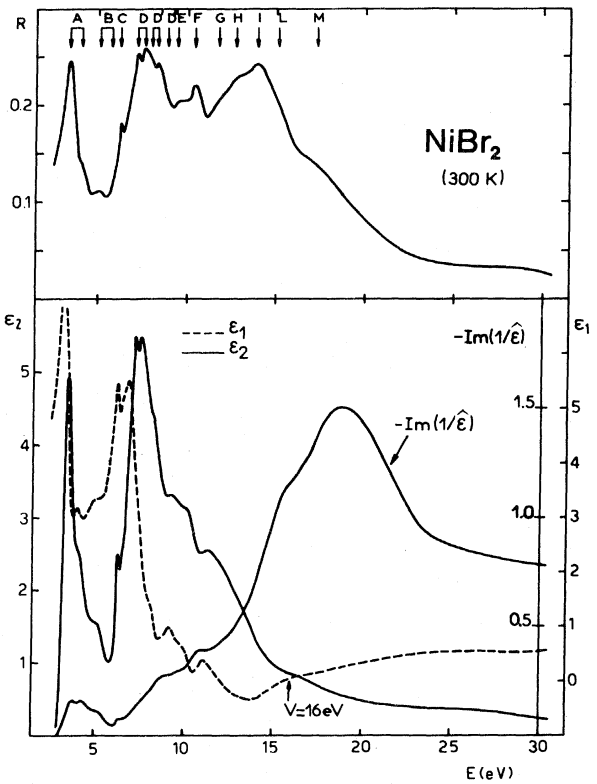

FIG. 2. Spectral dependence of the reflectance R, the real and imaginary parts of the dielectric constant ϵ_1 and ϵ_2, and the energy-loss function $-\mathrm{Im}(1/\hat{\epsilon})$ for $NiBr_2$ at room temperature.

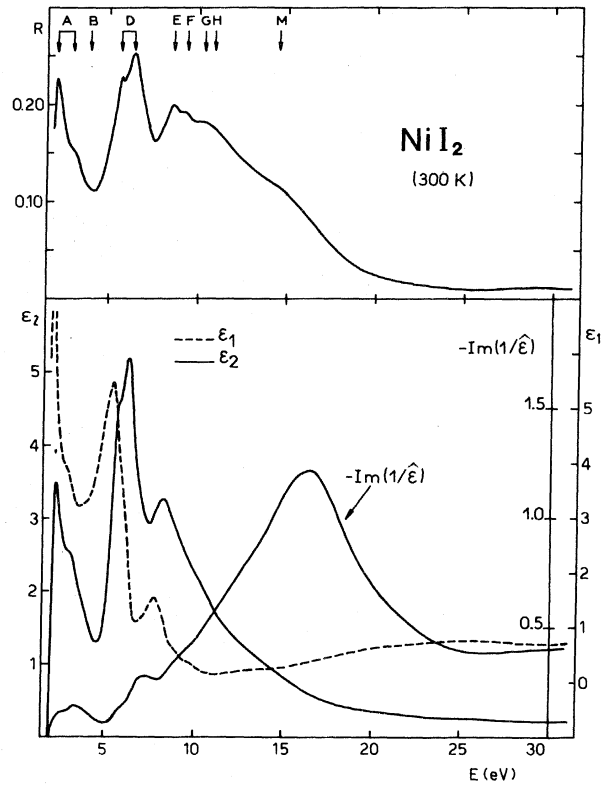

FIG. 3. Spectral dependence of the reflectance R, the real and imaginary parts of the dielectric constant ϵ_1 and ϵ_2, and the energy-loss function $-\mathrm{Im}(1/\hat{\epsilon})$ for NiI_2 at room temperature.

which for NiX_2 occurs in the range 16–21 eV. Since there is no corresponding feature in the $\epsilon_2(E)$ spectrum, and in addition, ϵ_1 and ϵ_2 are small[32] in the vicinity of the strong maximum and also have a positive and negative slope, respectively, it is reasonable to associate this energy loss with a somewhat broadened, many-electron or plasma excitation.

The plasma energy $\hbar\omega_p$ can be calculated from the maximum position of the imaginary part of $1/\hat{\epsilon}(E)$ [or $\epsilon_1(\hbar\omega_p)\simeq 0$; here nearly the same]. The values obtained by this way are around 20.2, 18.9, and 16.4 eV for $NiCl_2$, $NiBr_2$, and NiI_2, respectively, corresponding to the 16.3-, 15.1-, and 14.0-eV values calculated by the free-electron equation,

$$\omega_p^2=\frac{4\pi ne^2}{m}\ , \tag{1}$$

with n corresponding to six electrons per halide ion. However, it is probably a better approximation for the evaluation of plasma energies in insulators to take into account the presence of the energy gap, which shifts the plasmon energy from the free-electron value. In fact, the valence band is filled up by electrons and the conduction band is empty at 0 K, so that the organized plasma oscillations would be facilitated only by exciting electron-hole pairs. Thus the plasmon in insulators will be related, to some extent, to the exciton model. In this case, the plasmon energy for NiX_2 can be better estimated by the relation given by Horie,[16]

$$(\hbar\omega_p)^2\simeq(\hbar\omega_p)^2_{\mathrm{FE}}+E_g^2\ , \tag{1'}$$

where E_g is the energy gap between conduction and valence bands and $(\hbar\omega_p)_{\mathrm{FE}}$ is the free-electron (FE) plasmon energy. Now, if one considers the optical gaps of NiX_2 and calculates their free-electron plasmon energies only considering the p-halogen electron contribution (s electrons are very tightly bound to the atomic cores; they are 13–18 eV lower than the p valence band according to Antoci *et al.*[24]), one obtains the following values: $\hbar\omega_p\simeq 18.4$, 17.0, and 15.3 eV for $NiCl_2$, $NiBr_2$, and NiI_2, respectively, which are in reasonable agreement with experimental values (see Table I). Much of the experimental information concerning plasma oscillations comes from experiments of the characteristic energy losses suffered by electron beams scattered from both thin films and bulk crystals, from which one determines the function $-\mathrm{Im}[1/\hat{\epsilon}(E)]$, where the complex dielectric constant $\hat{\epsilon}$ refers to the longitudinal electron-electron interaction. The crystals studied are anisotropic and have tensorial dielectric functions, of which only the component $\epsilon_{xx}^T=\epsilon_{yy}^T$ has been measured.[4] Because the longitudinal and transverse dielectric response characteristics of photon-electron interactions can be shown to be very similar, within the random-phase approximation[33] and in the long-wavelength limit, it is of interest to compare directly the results of optical and characteristic energy-loss experiments carried out on $NiCl_2$ and $NiBr_2$.[34] In Fig. 7 of Ref. 34 are reported the characteristic electron-energy-loss

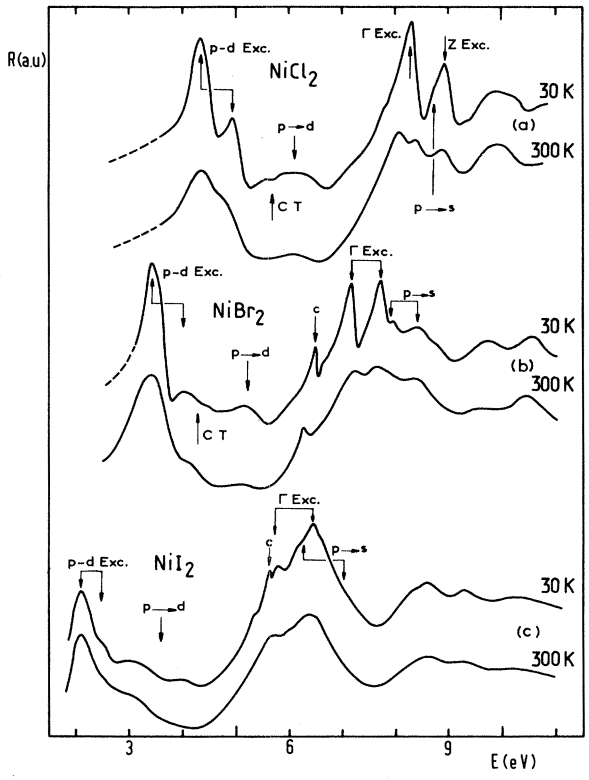

FIG. 4. (a)—(c) show details of the CT ($p \rightarrow d$) and exciton spectra of NiX_2 (X=Cl,Br,I) in the region of the fundamental absorption threshold ($p \rightarrow s$). For $NiCl_2$ and $NiBr_2$, an electron-energy loss is indicated, marked CT, with a value of, respectively, 5.7±0.2 and 4.2±0.1 eV, according to Best (Ref. 34).

spectra of iron, cobalt, and nickel halides. The energy-loss peaks marked CT (for charge transfer) and V, which are of interest to us, appear to have the same origin on account on their regular change in energy and relative intensity. The peaks labeled CT occur at 5.7±0.2 and 4.2±0.1 eV in $NiCl_2$ and $NiBr_2$, respectively, and are assigned to electron-transfer processes from the halide valence p shell to the nickel d shell. However, the energy losses labeled V have been associated with excitations of the valence-electron plasma oscillations, in agreement with calculated oscillation energy as described by Nozières and Pines.[15] For $NiCl_2$ and $NiBr_2$ the values reported for $\hbar\omega_p$ are 18 and 16.7 eV, respectively (see also Table VII of Ref. 34). When we compare the observed electron-energy losses V with optical data on nickel halides, we find a very acceptable agreement with the behavior of the function $-\mathrm{Im}[1/\hat{\epsilon}(E)]$. However, the maxima A,B in the reflectance spectra of $NiCl_2$ and $NiBr_2$ [see Figs. 4(a) and (b)] may be observed 0.5—1.0 eV below the reported CT energy-loss peaks. This difference can be accounted for by the fact that, for excitation of transitions at energies low compared with the plasma energy, the electron-energy loss is, in general, greater than the energy of the corresponding absorption maximum and has a reduced relative intensity.[15,35] A comparison of the theoretical and experimental results is summarized in Table I.

Returning to the low-energy structures A and B, or the higher-energy structures E and F (Fig. 4), we notice the great similarity of the spectra through the nickel halide family. Some differences are noticeable in the region where the sharp peaks C and D, and the faint structures D' occur. For example, the D peaks are strongly broadened passing from the bromides to the iodides, and the C peak, which probably has the same width in $NiBr_2$ and NiI_2, does not appear so well resolved in NiI_2 and is closer to the lower component of the D doublet than in $NiBr_2$: The energy distance of C is about 0.16—0.22 eV in NiI_2 compared to 0.65 eV in $NiBr_2$. This point will be commented upon in some detail in Sec. IV. Furthermore, in NiI_2, a small shoulder and one weak band are located around 6.26 and 7.15 eV, respectively (see Figs. 5 and 6).

In earlier works on alkali halides[17—19,21,36] it was considered, in general, that the existence of small shoulders, observed in most of the absorption and reflectance spectra, represents the onset of the lowest-energy interband transitions. Examples of such shoulders appear, for instance, around 7.8 eV in KBr or 6.2 eV in KI.[17,21] These shoulders, which are in many cases well separated from the much stronger exciton structure, have provided a basis for interpreting the interband scattering spectra. In $NiBr_2$, the positions of the spin-orbit-split shoulders in the low-temperature (30-K) spectrum of $\epsilon_2(E)$, the imaginary part of the dielectric constant, were found at about 7.90 and 8.39 eV, and were associated with the interband thresholds $\Gamma_3^-(\frac{3}{2}) \rightarrow \Gamma_1^+$ and $\Gamma_3^-(\frac{1}{2}) \rightarrow \Gamma_1^+$, respectively. Analogously, a slight indication of a shoulder in the 30-K spectrum of $\epsilon_2(E)$ was found at about 8.72 eV in $NiCl_2$ and associated with the $\Gamma_3^- \rightarrow \Gamma_1^+$ edge (see Figs. 5 and 6 of Ref. 4). In NiI_2 we can now suggest that the weak shoulder at 6.26 eV and the rather broad band around (7.10±0.05) eV might correspond to spin-orbit-split edges of the type $\Gamma_3^-(\frac{3}{2}), \Gamma_3^-(\frac{1}{2}) \rightarrow \Gamma_1^+$ (splitting approximately equal to 0.85 eV, close to the free-ion value of 0.95 eV). In addition to the shoulders representing interband scattering edges, we have to also consider the appearance of exciton states in the electronic spectra as a manifestation of the Coulomb interaction. Typical of excitonic features are the

TABLE I. Comparison of plasma frequencies (in eV) as given by free electrons $\hbar\omega_{p(\mathrm{FE})}$, the Horie relation $\hbar\omega_p$, the standard plasma dispersion relation $\epsilon_1(\omega_p) \simeq 0$; the maximum of energy-loss function from optical data $-\mathrm{Im}(1/\hat{\epsilon})_{\max}$, and electron-beam experiments.

	$\hbar\omega_{p(\mathrm{FE})}$	$\hbar\omega_p$	$\epsilon_1(\omega_p) \simeq 0$	$-\mathrm{Im}(1/\hat{\epsilon})_{\max}$	Energy loss
$NiCl_2$	16.3	18.4	16.7	20.2	18±0.2
$NiBr_2$	15.1	17.0	15.8	18.9	16±0.2
NiI_2	14.0	15.3	14.0	16.4	

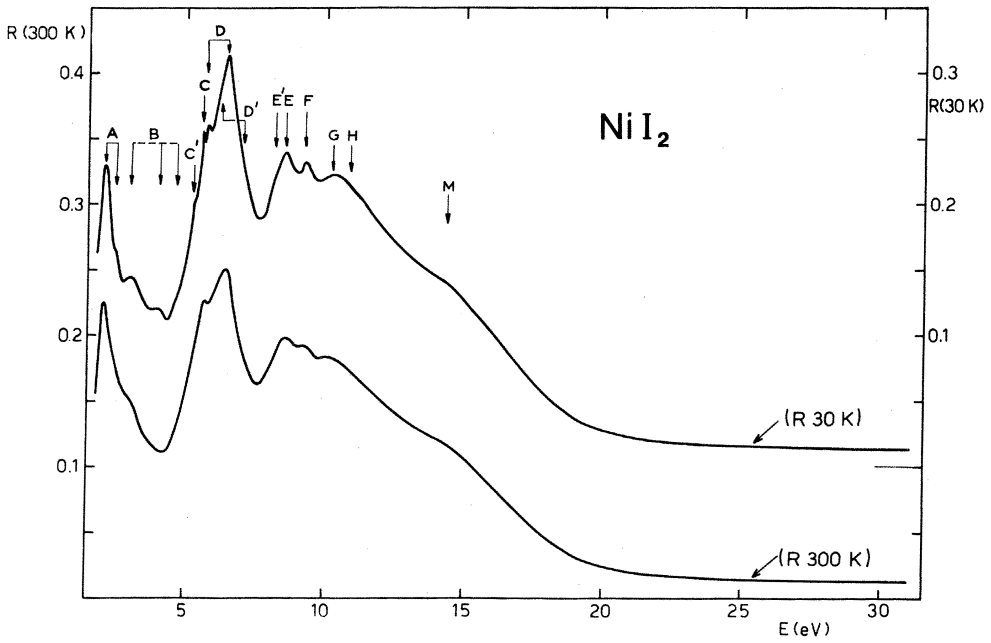

FIG. 5. Reflectance spectra of NiI_2 crystals at 300 and 30 K. The major structures discussed are designated A—M.

strong temperature dependence and the sharpness of the peaks compared to the interband structure. A connection with the exciton and interband spectra of alkali halides has been already anticipated,[4] since nickel halides may be considered a more complex version of the alkali halides, owing to the presence of d states in the forbidden energy band.

A comparison with the spectra of $MgCl_2$ and $MgBr_2$, which have the same layer-type crystal structure as the TMH's, is also of interest. Indeed, the spectra of these compounds[37] are similar to the TMH spectra as far as excitons and interband transitions are concerned; the $p \rightarrow d$ CT transitions of the TMH's (peaks A and B) are, of course, absent in $MgCl_2$ and $MgBr_2$. The foregoing connections also imply that the high-energy, badly broadened component of the D doublet located at 6.47 eV in NiI_2 should lie above the threshold for interband transitions, and thus its large width (0.8 eV) might partially be due to interaction with the continuum of states. Thus this strong peak is degenerate with direct transitions to band states,

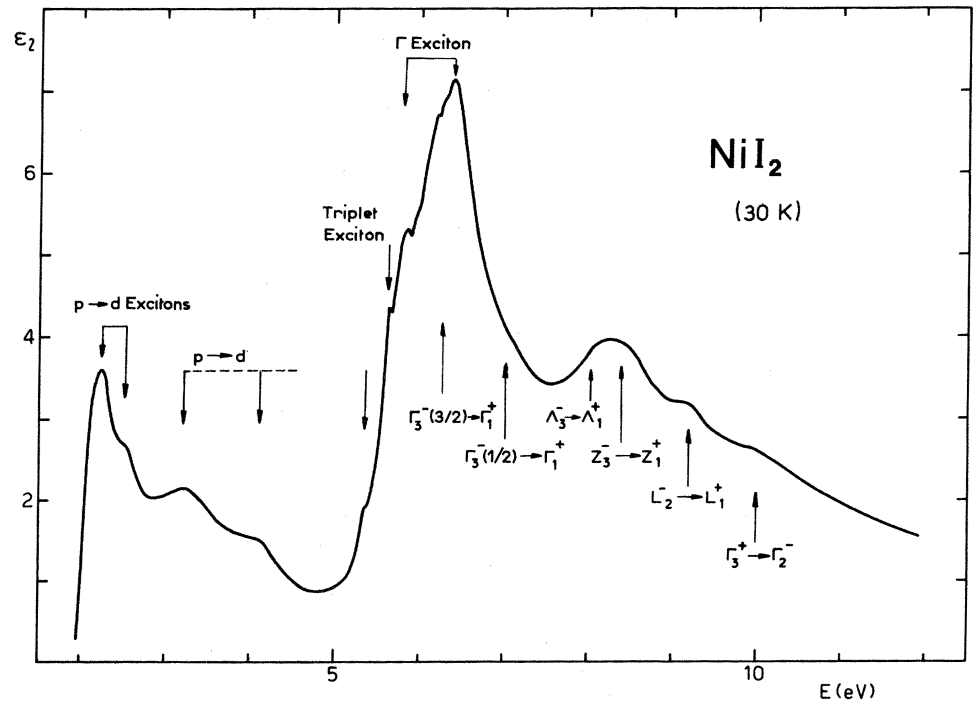

FIG. 6. Imaginary part of the dielectric constant of NiI_2, together with the proposed assignments.

which create free electrons and holes, as in alkali iodides. As a final consideration on NiI_2, we assign the peaks A_1 and A_2, located at 2.2 and 2.54 eV [see Figs. 4(c) and 6], to CT transitions to nickel d states, in agreement with the previous assignments made for the same peaks in $NiCl_2$ and $NiBr_2$.[3,4]

In Fig. 7 we show the plots of $n_{\text{eff}}(E)$, the effective number of electrons per NiX_2 molecule contributing to the optical absorption at photon energy E. The quantity is obtained from the sum rule

$$n_{\text{eff}}(E)=\frac{2m\epsilon_0 V}{\pi\hbar^2}\int_2^E E'\epsilon_2(E')dE' , \tag{2}$$

where m is the free-electron mass, V is the volume of unit cell (in Å^3), and E and E' are in eV. At higher energies, n_{eff} should finally saturate at a value of 20 corresponding to eight d electrons of the Ni ion and six valence electrons of the X ion of each NiX_2 molecule (assuming that deeper valence levels are not excited). Around 8 eV ($NiCl_2$), 7 eV ($NiBr_2$), and 6 eV (NiI_2), n_{eff} begins to increase to very high values, reaching 13.2 for $NiCl_2$, 14.3 for $NiBr_2$, and 13.6 for NiI_2. We think that the region of low n_{eff} values defines the CT region quite well. In fact, because of the small overlap between the halogen and the nickel d wave functions, CT transitions are allowed, but they are weaker than interband transitions. The sudden increase of n_{eff} should mark the onset of band-to-band transitions (and possible underlying orbital-promotion transitions). The fact that n_{eff} rises very quickly up to $E=12-15$ eV (passing from NiI_2 to $NiCl_2$) indicates that the optical transition strengths are strong in this spectral region, and shows, beyond this energy, a tendency towards saturation, which will probably be reached outside the spectral region studied, near 35–40 eV. In Fig. 7 we also report the values of the dielectric constant ϵ_{eff} determined by $\epsilon_2(E)$ over the entire spectral region of study,

$$\epsilon_{\text{eff}}(E)=1+\frac{2}{\pi}\int_2^E \frac{\epsilon_2(E')}{E'}dE' . \tag{3}$$

It is seen immediately that, beyond 13–15 eV (from NiI_2 to $NiCl_2$), the curves of NiX_2 saturate near the values of ϵ_{eff} (3.8 for $NiCl_2$, 4.0 for $NiBr_2$, and 4.4 for NiI_2), indicating that no further contribution to ϵ_{eff} from higher-energy transitions exists.

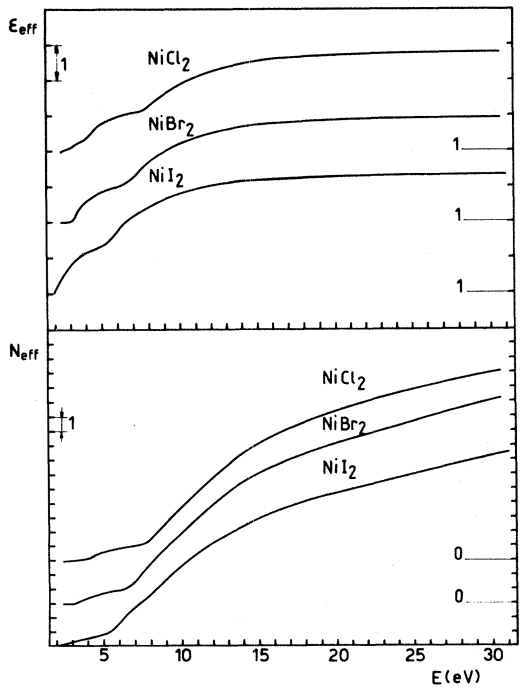

FIG. 7. Effective number of electrons per NiX_2 (X=Cl,Br,I) unit contributing to optical absorption. ϵ_{eff} is plotted vs photon energy for Ni halide insulators.

IV. DISCUSSION

In order to undertake the difficult task of identifying the optical structures observed in the low- and intermediate-energy region of the NiX_2 spectra, we will consider the known band structures determined by the intersecting-sphere model,[23,24] extending the interpretation reported for $NiCl_2$ and $NiBr_2$ (Ref. 4) to NiI_2. As noted in Sec. III the reflectance spectrum of NiI_2 is remarkably similar to that of $NiBr_2$ and $NiCl_2$, and, in addition, all crystals having the same $CdCl_2$ structure possess similar Brillouin zones. These facts, together with the overall resemblance of $NiCl_2$ and $NiBr_2$ band structures, suggest that the electronic structures for NiX_2 may differ only in minor respects, and therefore that a common band scheme should be quite adequate for a qualitative discussion of NiX_2 spectra. Furthermore, we have tried to obtain some knowledge from the comparison between soft-x-ray–absorption spectra of $NiCl_2$ (and TMC's) (Refs. 5, 25, and 26) and the corresponding optical response function $\epsilon_2(E)$. It is well known that soft-x-ray–absorption spectroscopy gives important information about the energy-band structures of solids. If one now compares the fundamental absorption spectra with the reported x-ray-absorption spectra for $NiCl_2$ (the $M_{2,3}$ absorption spectrum[27] is reported for $NiBr_2$), one finds that, although the spectral profiles are dissimilar among the different core-state spectra (i.e., Cl^- $L_{2,3}$, Cl^- K, and Ni $M_{2,3}$),[5,25–27] nevertheless some peaks have correspondences in the different spectra of a given material. This fact suggests that the structures should be caused by transitions to common final states of the excited electrons. It is this important circumstance that we are going to comment on carefully in order to obtain further information concerning the nature of the excitation mechanisms giving rise to optical structures in the vuv reflectance spectra.

First we discuss CT processes in which an electron is excited to an empty, metal d orbital. Such processes occur in the Ni $M_{2,3}$ absorption spectra studied in detail by Shin *et al.*;[5] the excitation leads to a final-state, $Ni^{2+}(3p^5 3d^9)$. These spectra are well explained by a localized excitation model with strong Coulomb and exchange interactions between Ni $3d$ electrons and the Ni $3p$ hole in the $Ni^{2+}(3p^5 3d^9)$ final state. Because of these strong final-state interactions, the $3d^9$ states in the presence of a $3p$ hole differ appreciably from the $3d^9$ states produced in vuv CT spectra (peaks A). Therefore the Ni $M_{2,3}$ spectra cannot be used in a simple manner for the interpretation of the vuv CT spectra.

The strong absorption peaks A of the Ni halides are attributed to a CT process of an electron from the valence band to a partially filled Ni $3d^8(e_g)$ orbital. We remark that the A peaks are much narrower than the width of the valence band (~ 5 eV). This indicates that the A peaks are due to the creation of excitons, bound states of a hole in the valence band, and an extra $3d(e_g)$ electron on Ni states. We attribute the broad absorption bands B to the corresponding band part, i.e., leading to (unbound) states with a hole in the valence band and an extra electron in the $3d(e_g)$ band of Ni. The fact that the absorption of band B extends over several eV corresponds to the combined width of the valence band and $3d(e_g)$ band. Since the $L_{2,3}$ shell ($2p$) of Cl^- and the valence band (mainly $3p$) have the same symmetry, and that, furthermore, the vuv and $L_{2,3}$ absorption have common final states for their transitions, it is expected that profiles of both L_2 and L_3 absorption bear a great resemblance to the corresponding vuv absorption. Transitions from the $L_{2,3}$ states to most principal points of the lower conduction bands are allowed. K absorption ($1s$), however, is generally ascribed to transitions to the p-type states in the conduction band. There is, however, some d-wave-function character on the halogen ion in both cases, and, furthermore, transitions can occur away from the "forbidden" critical points due to admixture of wave functions. We also note that the great similarity of K-absorption spectra and the similarity found between the calculated band structures of TMC's and $NiBr_2$ is consistent with the resemblance of vuv reflectance spectra noted above and is reassuring for our discussion.

In the following we shall refer to the band structure of NiX_2 (X=Cl,Br,I) shown in Fig. 8. The ordering and relative positions of the (valence-) conduction-band states for $NiCl_2$ are almost identical to those of $CoCl_2$ and $FeCl_2$ reported in Figs. 3–5 of Ref. 24, so we do not reproduce the corresponding band structures. We note that the band calculations show six valence bands of essentially halogen $3p$ character, five nickel d bands (displaying very small dispersion), and, above the d levels, we find an isolated conduction band, predominantly of Ni $4s$ character (dispersion about 2 eV), and three more bands of nickel with some admixture of p- and d-type states. Let us now discuss the observed Cl^- $L_{2,3}$ spectra of Fe, Co, and $NiCl_2$ shown in Fig. 7 of Ref. 26. These spectra consist of two parts: The low-energy region (below 210 eV) presents sharp absorption peaks to be associated with structures in the reflectance spectrum, and the high-energy region shows instead a rather broad and intense band, centered around 214 eV, to be associated with collective excitations[38] and probably corresponding to the reflectance peak M in $NiCl_2$. If the $L_{2,3}$ absorption curves of $NiCl_2$ (and also of TMC's) obtained by Sato *et al.*[26] are compared with the vuv spectrum of $NiCl_2$ (see Figs. 1 and 4), we find a rough agreement between the spectra in the sense that the double structures in the Cl^- $L_{2,3}$ spectra labeled A, B, D, and E should correspond to reflectance structures A, D_1, D_2, and E. Of course, when comparing soft-x-ray—absorption and vuv reflectance spectra, one must take into account the large 1.6-eV (Ref. 26) splitting of the chlorine $2p$ states, which in our case complicates the identification of corresponding structures. Let us first discuss the lowest-energy structures A and B in the Cl^- $L_{2,3}$ spectra. We note that there is a tendency that peak A shifts to low energy in a systematic manner from $MnCl_2$ to $NiCl_2$, while peak B lies at nearly fixed energy. The location of peak A also shifts in the same way in K-absorption spectra, shown in Fig. 1 of Ref. 25, and also in the ultraviolet absorption spectra.[2] If we now interpret the observed shift of the doublet A as the difference of the ionization energies of the divalent metal ions, we can identify the double peak A with transitions arriving at the partially filled d levels with creation of core holes in the $2p$ level of chlorine. The fixed doublet B in the Cl^- $L_{2,3}$ spectra can instead be attributed to transitions to the conduction-band minimum at Γ_1^+, with possible formation of excitons. Before coming to more detailed assignments based on NiX_2 band structures, we can now confirm the previous conclusions[4] for transitions occurring in the low- and intermediate-energy regions (peaks A–F) of the vuv spectra by stating that the most probable final state of the electron excited from the halogen p band, for A structures, are the unoccupied d levels of the nickel $3d^8$ ion, and, for structures D, E, and F, the final state is the $4s$ nickel level. If one accepts these arguments, then the doublet B is asso-

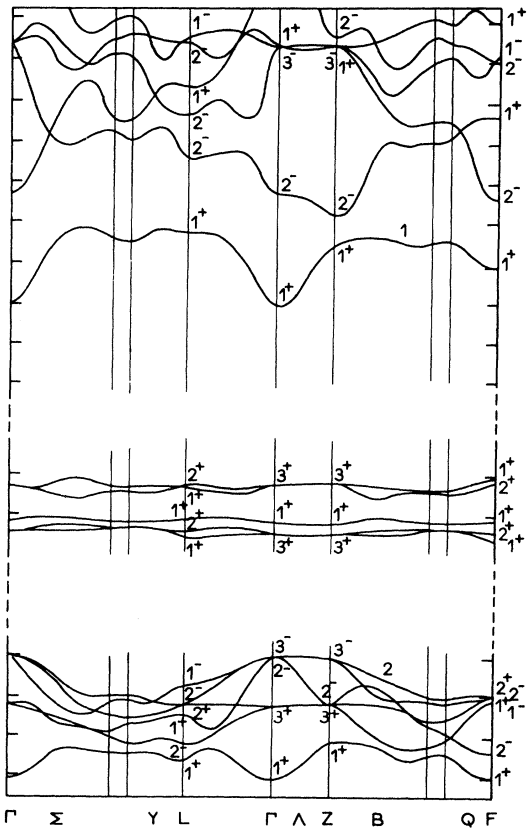

FIG. 8. Self-consistent band structure of $NiCl_2$ determined by the intersecting-sphere model according to Antoci and Mihich (Refs. 23 and 24). The forbidden gaps for $NiCl_2$ (and for NiI_2 or $NiBr_2$) have been purposely increased in order to reach agreement with the experimental values for interband transitions considered at the zone center and main symmetry points.

ciated with the transitions to Γ_1^+ (peak D_1) and the following peak is associated with transitions to the Z_1^+ level and the line Λ between Γ_1^+ and Z_1^+ (peaks D_2 and E). However, if one leaves the possible contribution of the saddle point Z_1^+ aside, then one could only associate the doublet D with the F_1^+ state at the zone-edge, with possible contribution of transitions along the symmetry line B. The assignment of the last doublet E in the Cl^- $L_{2,3}$ spectrum would correspond to either peak E or F of the reflectance spectrum of $NiCl_2$, depending on the choice of the previous assignments. Furthermore, we note that the vuv spectra of NiX_2 present more structures than one can observe in the Cl^- $L_{2,3}$— (and K-) absorption spectra. These spectra present a minimum of absorption about 7—8 eV above the doublet B, which finds its counterpart in a dip in the theoretical density of states[24] and in the beginning of the smooth decrease of the reflectivity beyond the structure L. An intriguing feature of the $L_{2,3}$ spectra is the complete absence of structure between F and L. This could be due to a relatively strong excitonic contribution to the Cl^- $L_{2,3}$ spectra; the Coulomb interaction between the Cl($2p$) hole and the conduction-band electron leads to a large intensity for the exciton, thereby strongly reducing the band part. In the vuv spectra a Cl($3p$) hole is produced; this hole has a larger spatial extension than the Cl($2p$) hole and will have a smaller Coulomb interaction with the excited electron in the conduction band. Therefore we expect a larger exciton contribution and a smaller band contribution for the Cl^- $L_{2,3}$ spectra than for the vuv absorption spectra. This may explain the reduced intensity at the high-energy side (band part) of Cl^- $L_{2,3}$ spectra as compared to vuv spectra. Of course, owing to the uncertainty due to the exchange approximation and the influence of the exciton interaction, we cannot safely identify all the high-energy structures (from F to L), shown in Figs. 1—3, beyond qualitative information concerning the energy range. For this reason we discuss in some detail only the case of $NiCl_2$, for which there is more experimental and theoretical support, leaving to the reader the generalization to the similar cases of $NiBr_2$ and NiI_2. To this end we summarize in Table II all the experimental results and the assignments made by considering the optically allowed transitions starting from the uppermost Cl valence bands to the conduction bands with various irreducible representations (1^+,2^-,...) at the high-symmetry points in the Brillouin zone (see Fig. 8). It is found, by x-ray photoemission spectra, that the width of the valence band is about 5 eV for $NiCl_2$ and $NiBr_2$. Of course, in photoemission experiments the valence states of NiX_2 consist of the $3d$ states of Ni and the np states of halogen, n being 3, 4, and 5 for chlorine, bromine, and iodine, respectively. For $NiCl_2$ the width of the p valence region is 4.3 eV when $\alpha=\frac{2}{3}$ and 3.2 eV when $\alpha=1$ (Slater approximation); the gap between the valence Γ_3^- level and the Γ_1^+ conduction minimum is 4.1 eV for $\alpha=\frac{2}{3}$ and 5.9 eV for $\alpha=1$.[24] Therefore, we shall hereafter adopt the results of the calculated band structures with the Slater approximation for the exchange potential. Of course, the energy separation between the top of the valence band and the bottom of the conduction band at point Γ is assumed to be about 8.70 eV for $NiCl_2$, the experimentally obtained energy gap. The same procedure is followed for $NiBr_2$ and NiI_2 in order to evaluate the transition energies reported in Table II.

Interband transitions begin at 8.72 eV with a M_0-type critical point produced by the $\Gamma_3^- \rightarrow \Gamma_1^+$ transition. In the experimental reflectance data we see that the fundamental gap is between excitons Γ and Z [see Figs. 4(a) and 6 of Ref. 4]. The exciton peaks are rather large and their existence peaks are rather large and their existence weakens the interband transition. The following band-to-band transitions take place along the symmetry line Λ and at the Z point ($Z_3^- \rightarrow Z_1^+$). We assign the D_2' peak at 9.9 eV and the E peak at 10.2 eV in Figs. 1 and 4(a) (see also Fig. 2 of Ref. 4) to these transitions. The next band-to-band transition arises at the F point, that is, the $F_2^- \rightarrow F_1^+$ (10.7 eV). We assign peak F at 10.8—11.0 eV to that transition. We then see, in Table II and Fig. 1, that the energies of the band-to-band transitions at $\Gamma(\Gamma_3^+ \rightarrow \Gamma_2^-)$, $F(F_2^- \rightarrow F_1^+,\ F_1^+ \rightarrow F_2^-)$, $Z(Z_3^+ \rightarrow Z_2^-)$, and $L(L_2^- \rightarrow L_1^+, L_1^+ \rightarrow L_2^-)$ cover the $\sim$(11—15)-eV energy region. Thus these transitions may be assigned to the peaks G, H, and I of $NiCl_2$. The structure L (15.4 eV) is presumably due to $\Gamma_3^- \rightarrow \Gamma_1^+$ (15.2 eV), whereas the structure M (18.3 eV) is assigned to $\Gamma_1^+ \rightarrow \Gamma_3^-$ (18.2 eV) from inner-valence-band state Γ_1^+ to higher-conduction-band state Γ_3^-. The weak structure N is assigned to the possible ionization of the chlorine valence s shell.[34] Starting from the optical structure G, the peaks and structures occurring in the reflectance spectrum of $NiCl_2$ should originate from the gap between the Cl and Ni inner-valence-band states and the lower Ni and Cl p and s levels. These tentative assignments, which agree reasonably well with the calculated band structure, are reported in Table II for the various transitions; the analogous assignments for $NiBr_2$ NiI_2 are reported in Table II and Fig. 6.

The final part of the discussion concerns the satellite exciton (peak C in Figs. 2, 4, 5, and 9) occurring in $NiBr_2$ and NiI_2. In alkali halides the ratio of the integrated intensities for the doublet excitons should be roughly equal to 2:1, proportional to the multiplicity of the valence states. However, it is a usual outcome of experiments that this theoretical prediction is not satisfied in most of the cases: For example, if we consider the ratio of the integrated intensities of the first $(\frac{3}{2},\frac{1}{2})$ and the second $(\frac{1}{2},\frac{1}{2})$ peaks for NaBr, KBr, or RbBr,[17,39] we find values of 0.45, 0.69, and 1.06, which are rather smaller than 2, and sometimes the second-exciton peak is even stronger than the first-exciton peak.[17,21] A detailed discussion of the effects of spin-orbit and electron-hole interactions on exciton states was given long ago by Onodera and Toyozawa.[39] In particular, they pointed out that one can have, in addition to optically allowed singlet states (actually mixtures of singlet and triplet states), pure (zero-phonon) triplet states, which are forbidden, in principle, in a direct optical process. However, this selection rule can be relaxed in the presence of an exciton-phonon interaction which mixes the pure triplet state with the allowed singlet states, and thus makes the transition to triplet states partially allowed. In principle, there are sound reasons which make the experimental detection of the triplet exciton, which is theoretically situated on the low-energy side of

TABLE II. Energies of the structures in the imaginary part of the dielectric constant ϵ_2 and reflectance (R) spectra observed at 300 K in $NiCl_2$ and $NiBr_2$, and at 30 K in NiI_2. These experimental energies are compared with the theoretical values of possible assignments in connection with the calculated band schemes. (Exc. denotes exciton.)

	$NiCl_2$			$NiBr_2$			NiI_2		
Label	R	ϵ_2	Theor.	Label	R	ϵ_2	Theor.	Label	R	ϵ_2	Theor.
D_1	8.07	8.07	Exc. Γ	C	6.27	6.30	Exc.	C'	5.33	5.36	Exc.
D_1'	8.73	8.72	$\Gamma_3^- \rightarrow \Gamma_1^+$ = gap	D	7.20	7.20	Exc. Γ	C	5.62	5.65	Exc.
D_2	8.85	8.80	Exc. Z	D	7.64	7.60	Exc. Γ	D_1	5.79	5.82	Exc. Γ
D_2'	9.9	9.8	Λ line	D'	7.82	7.8	$(\frac{3}{2})\Gamma_3^- \rightarrow \Gamma_1^+$ = gap	D_2	6.47	6.40	Exc. Γ
E	10.2	10.1	$Z_3^- \rightarrow Z_1^+$ = 10.3	D'	8.3	8.3	$(\frac{1}{2})\Gamma_3^- \rightarrow \Gamma_1^+$ = gap	D_1'	6.3	6.3	$(\frac{3}{2})\Gamma_3^- \rightarrow \Gamma_1^+$ = gap
F	10.8	10.8	$F_2^- \rightarrow F_1^+$ = 10.7	E	9.4	9.4	$Z_3^- \rightarrow Z_1^+$ = 9.4	D	7.15	7.14	$(\frac{1}{2})\Gamma_3^- \rightarrow \Gamma_1^+$ = gap
G	11.9	11.8	$L_2^- \rightarrow L_1^+$ = 11.7	F	10.4	10.3	$F_2^- \rightarrow F_1^+$ = 9.9	E'	8.2	8.2	Λ line
			$Z_3^+ \rightarrow Z_2^-$ = 12.1				$L_2^- \rightarrow L_1^+$ = 10.8	E	8.6	8.5	$Z_3^- \rightarrow Z_1^+$ = 7.8
H	13.3	13.1	$\Gamma_3^+ \rightarrow \Gamma_2^-$ = 12.7	G	11.7	11.5	$F_1^+ \rightarrow F_2^-$ = 11.5				$F_2^- \rightarrow F_1^+$ = 8.3
			$L_1^+ \rightarrow L_2^-$ = 13.8				$L_2^- \rightarrow L_1^+$ = 11.8	F	9.3	9.2	$L_2^- \rightarrow L_1^+$ = 9.2
I	14.3	13.7	$F_1^+ \rightarrow F_2^-$ = 14.3	H	12.6	12.4	$\Gamma_3^- \rightarrow \Gamma_2^-$ = 11.9				$Z_3^+ \rightarrow Z_2^-$ = 9.7
			$F_2^- \rightarrow F_1^+$ = 14.4				$L_1^+ \rightarrow L_2^-$ = 13.0	G	10.2	10.0	$\Gamma_3^+ \rightarrow \Gamma_2^-$ = 10.2
L	15.4	15.0	$\Gamma_3^- \rightarrow \Gamma_1^+$ = 15.2	I	13.9	13.6	$F_1^+ \rightarrow F_2^-$ = 13.5				$L_2^- \rightarrow L_1^+$ = 10.2
			$L_2^- \rightarrow L_1^+$ = 15.3				$F_2^- \rightarrow F_1^+$ = 13.6	H	10.8	10.6	$L_1^+ \rightarrow L_2^-$ = 11.3
M	18.3	18.0	$Z_1^+ \rightarrow Z_3^-$ = 17.3	L	15.1	14.9	$F_2^- \rightarrow F_1^+$ = 15.0	M	14.4	14.0	$F_2^- \rightarrow F_1^+$ = 14.2
			$\Gamma_1^+ \rightarrow \Gamma_3^-$ = 18.2				$L_1^+ \rightarrow L_2^-$ = 15.2				$Z_1^+ \rightarrow Z_3^-$ = 14.8
N	22.8	22.8		M	16.8	16.5	$Z_1^+ \rightarrow Z_3^-$ = 16.5				

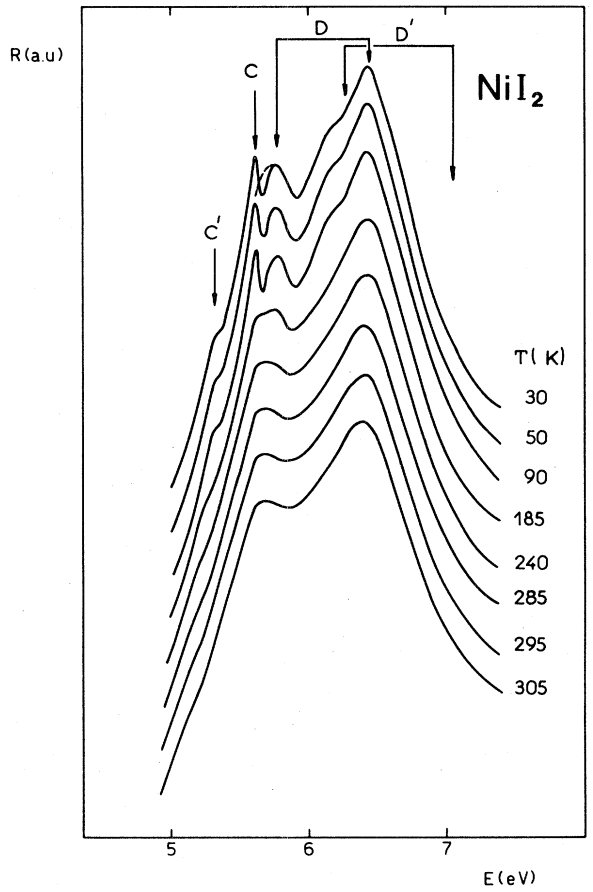

FIG. 9. Reflectance spectra of NiI_2 taken at fixed temperatures between 305 and 30 K in the excitonic energy range.

the $(\frac{3}{2},\frac{1}{2})$ exciton, difficult; that is, (i) the expected low intensity for the triplet exciton, and (ii) the energy separation between triplet and singlet excitons (dependent on the exchange energy Δ and the spin-orbit splitting λ) may be small. The latter consideration seems to exclude the observation of triplet excitons in the TMC's, where the estimated triplet-singlet separation ($\sim$0.03 eV) is too small. In TMB's, on the other hand, the triplet state could be separated by 0.15 eV or more from the first component of the Γ exciton, so that it could be possible, in principle, to observe a phonon-assisted exciton structure. In effect, Petroff and co-workers,[40] by means of careful reflectivity measurements 1.8 K from very clean surfaces of KI, have reported an indirect observation of the zero-phonon triplet exciton. In fact, they observed the first phonon sideband 10 meV lower in energy from the $n=1$ exciton. In $NiBr_2$,[4] on the other hand, due to the presence of d states in the forbidden gap, there exists a strong background below the Γ doublet, formed by the preceding CT transitions, where an intensity-stealing process can successfully transfer a large oscillator strength to transitions to the excitonic triplet state by means of a strong exciton-phonon interaction (30 K). In this case a true exciton resonance (peak C), whose line shape shows the typical asymmetry and antiresonance caused by interference with the scattering background, is observed at 6.5 eV, well separated from the 7.15-eV exciton (peak D). The intensity ratio of the two components of the Γ-exciton doublet in $NiBr_2$ is of the order of unity. Applying the arguments developed by Onodera and Toyozawa to TMH's, this corresponds to an intermediate exchange interaction in $NiBr_2$, which reduces the width of the first excitonic (singlet) peak ($\Gamma\sim0.3$ eV) by interband scattering with the excitonic triplet state C ($\Gamma_c\sim0.15$ eV), so that the magnitude of the width of the first and second ($\Gamma_D\sim0.4$ eV) components of the Γ exciton would become of the same order of magnitude. In NiI_2 the intensity ratio is around 1:2, which would imply a larger exchange interaction. This is theoretically expected since the exchange energy is more largely dependent on the halogen ion than on the metal ion. Yet, it is not clear whether the large intensity transfer between the doublet component would also involve a larger value for the singlet-triplet energy separation than the value found ($\simeq$0.2 eV). In fact, we found that the relevant experimental parameters for the Γ excitons can be explained quite well by the theory of Onodera and Toyozawa for NiI_2, but not so well for $NiBr_2$. For example, if we use $\Delta=0.43$ eV and $\lambda=0.60$ eV for NiI_2, we calculate, for the C-D splitting of the triplet exciton, 0.23 eV, which is very near to the observed value of 0.2 eV.

However, for $NiBr_2$ it seems difficult to fit a C-D distance of 0.65 eV, a spin-orbit splitting of the exciton of about 0.5 eV, and an intensity ratio of 1:1 with reasonable values of Δ and λ. One more point worthy of consideration is the temperature behavior of peak C in $NiBr_2$ (see Fig. 3 of Ref. 4) and in NiI_2 (Fig. 9). We see that in NiI_2 the energy position of peak C is rather fixed versus temperature, while in $NiBr_2$ a thermal behavior of peak C is observed. We now expect that the temperature may slightly alter the exchange energy; however, we do not find physical reasons for the puzzling behavior of these two C peaks. These points cast a shadow on the interpretation of the origin of peak C in $NiBr_2$.

In conclusion, even though one feels that the qualitative explanation offered for the appearance of the satellite exciton in nickel halides may be likely and sound, the points concerning the energy distance of the triplet exciton and its temperature behavior seem difficult to understand in $NiBr_2$ and require careful consideration. It is suggested that a new treatment in which the spin-orbit and exchange interactions are taken into account for TMH's in the calculations of the model could cast some light on the present difficulties.

V. SUMMARY AND CONCLUSIONS

We have measured the reflectance spectra of NiX_2 and used dispersion analysis to generate the ϵ_2 and $-\mathrm{Im}[1/\hat{\epsilon}(E)]$ functions over the entire energy region 2–31 eV. The similarity between the spectra suggests that their interpretation can be attempted on the basis of a self-consistent band structure of $NiCl_2$ and $NiBr_2$, provided that the band-gap value is empirically adjusted. On this basis, nearly all of the main spectral features below 12–15 eV can be identified in terms of CT, exciton, and direct interband transitions. In particular, the prominent low-energy features of the NiI_2 spectrum, reported here

for the first time, are identifiable as in the case of $NiCl_2$ and $NiBr_2$. The careful discussion based on the results of the band-structure calculations of $NiCl_2$ and TMC's, and known soft-x-ray—absorption spectra of these materials, has suggested an unique interpretation of the features occuring in vuv spectra. Along these lines, it appears that the peaks occuring just above the threshold of NiX_2 (from 6.3 to 8.7 eV) should be assigned to direct transitions betwen the halogen p levels and the metal s levels, while the structure in the intermediate-energy region should be derived from transitions between deeper halogen p and s levels and upper metal p and d levels. Plasma resonance effects occur in all materials and have been confirmed from the $-\mathrm{Im}[1/\hat{\epsilon}(E)]$ function, which presents broad and intense maxima in the region of 16—21 eV. The optical data have been found to be in good agreement with the directly measured electron-energy losses. Finally, we have discussed the appearance of satellite excitons in $NiBr_2$ and NiI_2 and the possible existence of a forbidden triplet exciton state below the first allowed exciton state of the Γ doublet in NiI_2. The same interpretation for $NiBr_2$ seems more doubtful at the present moment.

ACKNOWLEDGMENTS

The authors thank the technical staff of the Laboratoire d'Utilisation du Rayonnement Electromagnétique, as well as the members of the Laboratoire de l'Accélérateur Linéaire (Orsay), for providing the Armeau de Collision d'Orsay beam facilities during the course of the experiment. One of us (I.P.) gratefully acknowledges the Centre National de la Recherche Scientifique for financial support during his stay at the University of South Paris. Finally, all of us are grateful to Professor C. Haas for many helpful discussions. This investigation was supported in part by the Netherlands Foundation for Chemical Research (SON) with financial aid from the Netherlands Organization for the Advancement of Pure Research (ZWO).

[1]T. Ishii, Y. Sakisaka, T. Matsukawa, S. Sato, and T. Sagawa, Solid State Commun. 13, 281 (1973).

[2]Y. Sakisaka, T. Ishii, and T. Sagawa, J. Phys. Soc. Jpn. 36, 1365 (1974); Y. Sakisaka, *ibid.* 38, 505 (1975).

[3]G. Guizzetti, L. Nosenzo, I. Pollini, E Reguzzoni, G. Samoggia, and G. Spinolo, Phys. Rev. B 14, 4622 (1976).

[4]I. Pollini, J. Thomas, G. Jezequel, J. C. Lemonnier, and R. Mamy, Phys. Rev. B 27, 1303 (1983); I. Pollini, G. Benedek, and J. Thomas, *ibid.* 29, 3617 (1984).

[5]S. Shin, S. Suga, M. Taniguchi, H. Kanzaki, S. Shibuya, and T. Yamaguchi, J. Phys. Soc. Jpn. 51, 906 (1982).

[6]R. J. Powell and W. E. Spicer, Phys. Rev. B 2, 2182 (1970).

[7]D. L. Greenaway and R. Nitsche, J. Phys. Chem. Solids 26, 1445 (1965); D. K. Wright and M. R. Tubbs, Phys. Status Solidi 37, 551 (1970).

[8]S. Kondo and H. Matsumoto, J. Phys. Soc. Jpn. 51, 1441 (1982).

[9]K. Kanzaki and I. Imai, J. Phys. Soc. Jpn. 32, 1003 (1972).

[10]R. H. Bube, Phys. Rev. 106, 703 (1957).

[11]D. L. Greenaway and G. Harbeke, J. Phys. Soc. Jpn. 21, 151 (1966); G. Harbeke and T. Tosatti, Phys. Rev. Lett. 28, 1567 (1972).

[12]H. Fesefeldt, Z. Phys. 64, 741 (1930).

[13]M. R. Tubbs, J. Phys. Chem. Solids 29, 1191 (1968).

[14]D. Brust, Phys. Rev. 134, A1337 (1964).

[15]P. Nozières and D. Pines, Phys. Rev. 113, 1254 (1959); 109, 741 (1958); 109, 1062 (1958); D. Pines, Rev. Mod. Phys. 28, 184 (1956).

[16]L. Marton, Rev. Mod. Phys. 28, 172 (1956); C. Horie, Prog. Theor. Phys. 21, 113 (1959).

[17]J. E. Eby, K. J. Teegarden, and D. B. Dutton, Phys. Rev. 116, 1099 (1959).

[18]R. S. Knox and N. Inchauspé, Phys. Rev. 116, 1093 (1959).

[19]H. R. Philipp and H. Ehrenreich, Phys. Rev. 129, 1550 (1963).

[20]H. R. Philipp and H. Ehrenreich, Phys. Rev. 131, 2016 (1963).

[21]K. Teegarden and G. Baldini, Phys. Rev. 155, 896 (1967); G. Baldini and B. Bosacchi, *ibid.* 166, 863 (1968).

[22]G. W. Rubloff, Phys. Rev. B 5, 662 (1972).

[23]S. Antoci and L. Mihich, Phys. Rev. B 18, 5768 (1978).

[24]S. Antoci and L. Mihich, Phys. Rev. B 21, 3383 (1980).

[25]C. Sugiura, J. Phys. Soc. Jpn. 33, 455 (1972).

[26]S. Sato, T. Ishii, I. Nagakura, O. Aita, S. Nakai, M. Yokota, K. Ichikawa, G. Matsuoka, S. Kono, and T. Sagawa, J. Phys. Soc. Jpn. 30, 459 (1971).

[27]S. Nakai, H. Nakamori, A. Tomita, K. Tsutsumi, N. Nakamura, and C. Sugiura, Phys. Rev. B 9, 1870 (1974).

[28]S. Hüfner and G. K. Wertheim, Phys. Rev. B 8, 4857 (1973); G. K. Wertheim, H. J. Guggenheim and S. Hüfner, Phys. Rev. Lett. 30, 1050 (1973).

[29]Y. Sakisaka, T. Ishii, and T. Sagawa, J. Phys. Soc. Jpn. 36, 1372 (1974).

[30]T. Ishii, S. Kono, S. Suzuki, I. Nagakura, T. Sagawa, R. Kato, M. Watanabe, and S. Sato, Phys. Rev. B 12, 4320 (1975); C. Sugiura, *ibid.* 9, 2679 (1974).

[31]S. R. Kuindersma, Phys. Status Solidi B 107, K163 (1981); S. R. Kuindersma, J. P. Sanchez, and C. Haas, Physica 111B, 231 (1981).

[32]H. Fröhlich and H. Pelzer, Proc. Phys. Soc. London, Sect. A 68, 525 (1955). In fact, the condition for the existence of plasma oscillations at frequency ω is just $\tilde{\epsilon}(\omega)=0$; this equation is solved, in the general case, by a complex frequency whose real part corresponds to the plasma frequency and whose imaginary part corresponds to the damping of the plasma resonance.

[33]S. L. Adler, Phys. Rev. 126, 413 (1962).

[34]P. E. Best, Proc. Phys. Soc. London 80, 1308 (1962).

[35]H. Frölich, *Max-Planck Festschrifts* (Deutschen Verlag, der Wissenschaften, Berlin, 1958), Vol. 277.

[36]The important structure in the valence band is determined by the spin-orbit parameter λ. This can be estimated from the splitting of the free-halogen doublet by $\frac{3}{2}\lambda$ (Ref. 17). The spin-orbit parameter λ for the p valence states of the free-halide-atoms are 0.07, 0.31, and 0.63 eV for Cl, Br, and I, respectively.

[37]S. Kinno and R. Onaka, J. Phys. Soc. Jpn. 49, 1379 (1980); 50, 2073 (1981).

[38]F. C. Brown, C. Gähwiller, H. Fujita, A. B. Kunz, W. Scheifley, and N. Carrera, Phys. Rev. B 2, 2126 (1970); H. Fujita, C. Gähwiller, and F. C. Brown, Phys. Rev. Lett. 22, 1369 (1969).

[39]Y. Onodera and Y. Toyozawa, J. Phys. Soc. Jpn. 22, 833 (1967).

[40]Y. Petroff, R. Pinchaux, C. Chekroun, M. Balkanski, and H. Kamimura, Phys. Rev. Lett. 27, 1377 (1971).